Effect of Crystallization Behavior of Polyethylene Glycol 6000 on the Properties of Granules Prepared by Fluidized Hot-Melt Granulation (FHMG)

Motonori KIDOKORO,* Kaoru SASAKI, Yasuo HARAMIISHI, and Norio MATAHIRA

Shizuoka Pharmaceutical Research Center, Pharmaceutical Technology Research Laboratories, Daiichi Pharmaceutical Co., Ltd.; 588 Kanaya-kawara, Kanaya-cho, Haibara-gun, Shizuoka 428–0021, Japan.
Received October 8, 2002; accepted February 26, 2003

The objective of this study was to investigate the effect of the crystallization behavior of Macrogol 6000 (polyethylene glycol 6000; PEG 6000), used as a binder, during the solidification process on the properties of mononucleic granules prepared by the fluidized hot-melt granulation (FHMG) technique. Crystallization of PEG 6000 from molten liquid was investigated using differential scanning calorimetry (DSC) and hot stage microscopy. The results obtained from the measurement of isothermal crystallization demonstrated that crystallization of PEG 6000 was either slow or rapid. Analysis based on solid-state decomposition showed that slow crystallization was due to the two-dimensional growth of nuclei mechanism, while rapid crystallization was due to the three-dimensional growth of nuclei mechanism. Observation of the crystallization of PEG 6000 by hot stage microscopy supported the existence of two different crystallization mechanisms. Granules containing PEG 6000 that underwent rapid crystallization during FHMG showed a significantly higher fraction powder under 150 μm in diameter. This was caused by the loss of powder particles from the surface of mononucleic granules during the solidification process, because many cracks were observed after crystallization of PEG 6000 with a short isothermal crystallization time (ICT) due to the reduced of sticking of particles. The results of this study suggested that the crystallization behavior of the binder during the solidification process of FHMG can influence the properties of the resultant granules, such as particle size distribution, content uniformity or taste masking. It was also indicated that measuring the ICT using DSC was a useful method to classify PEG 6000.

Key words polyethylene glycol 6000; fluidized hot-melt granulation; crystallization; granules

Granulation is one of the most important processes in pharmaceutical manufacturing. Powders show improved flowability and content uniformity as a result of granulation. Hot-melt granulation (HMG), using meltable materials as thermal binders, is classified as a dry granulation method. HMG is a well-known granulation technique that utilizes adhesion due to the melting or softening of materials that are heated to near or above their melting point.[1] Currently, HMG is of great interest in the pharmaceutical field, since granules may be prepared simply without using solvents or water. HMG is also a very useful method for granulating and stabilizing drugs that are susceptible to hydrolysis.[2] Ukita and Murakami demonstrated that melt granulation prevented the vaporization of essential oils during the granulation process because the melted material covered the surface of the granules.[3] The melt granulation process can also be applied to prepare sustained-release dosage forms of drugs. Maejima *et al.* developed the tumbling melt granulation (TMG) technique, which is a type of powder coating method using hydrophobic melting materials for the production of sustained-release beads.[4—6] Faham *et al.* investigated hot-melt coating technology using a spray system.[7] In addition, this technique has advantages for scaling-up and process validation because there are only a few controlling parameters.[8]

Conventional HMG is performed in a high shear mixer or a tumbling mixer with almost 30 w/w% of low melting point material and other powder excipients. As a result, granules prepared by the HMG method are dense and very hard, having a sand-like feeling. Therefore, this method was not thought to be good for making preparations of granules and fine granules as defined by the Japanese Pharmacopoeia XIV.

On the other hand, we have developed fluidized hot-melt granulation (FHMG), a novel, simple, and useful method of preparing granules without using solvents or water.[9—12] This technique is also easily controlled, so we have investigated its usefulness in the field of pharmaceutical formulation and production technology.[9] In general, fluidized bed granulation is a suitable method to prepare fine granules as well as granules for tabletting, because the lack of any shear force during granulation results in porous granules with a low strength.[13,14] Our studies have also shown that granules prepared by the FHMG method are softer compared with those obtained by the conventional HMG method. In previous studies, FHMG has been shown to have the capability to make fine, taste-masked granules containing a bitter drug substance,[11] as well as being useful for making granules for tabletting.[15] Schæfer *et al.* studied the effect of process[16,17] and formulation variables[18—20] on melt granulation with low molecular weight PEGs using a high shear mixer. Voinovich *et al.* also investigated the effect of the apparatus and the process variables during melt pelletization using a high shear mixer.[21] Haramiishi *et al.* reported a formulation study and the mechanism of obtaining mononucleic granules with a high yield by FHMG.[9] However, most studies have concentrated on formulation and have been performed to investigate the granulation mechanism or the optimum conditions. Thus, few reports have described the solidification process of melting materials during HMG.

The objective of the present study was to investigate the effect of the crystallization behavior of Macrogol 6000 (polyethylene glycol 6000; PEG 6000), which is used as a binder, during the solidification process on the properties of mononucleic granules prepared by a FHMG. The crystallization behavior of PEG 6000 from molten liquid was investi-

* To whom correspondence should be addressed. e-mail: kidokknl@daiichipharm.co.jp

gated using differential scanning calorimetry (DSC) and hot stage microscopy. The process of isothermal crystallization was analyzed by a solid-state decomposition method.[22,23] Granules produced by the FHMG technique were also evaluated.

Experimental

Materials Macrogol 6000 (polyethylene glycol 6000; PEG 6000, NOF Corp., Tokyo, Japan) was of JP grade. PEG 6000 was pulverized by a sample mill, and then sieved. The fraction obtained between the 180 μm and 250 μm screens was used for granulation. Cetraxate hydrochloride (CET, Daiichi Pharm. Co., Ltd.) was used as a model drug. α-Lactose monohydrate 450 mesh (Pharmatose 450 M) was purchased from DMV (Veghel, The Netherlands). The other materials used were corn starch (Nihon Shokuhin Kako Co. Ltd., Tokyo, Japan) and talc (Matsumura Sangyo Co. Ltd., Osaka, Japan).

Methods. FHMG Granules were prepared by the FHMG technique using a fluidized-bed system (FLO-1, Freund Industrial Co. Ltd., Tokyo, Japan). Table 1 shows the formulations employed for FHMG. The content of PEG 6000 as a binder was fixed at 25 w/w % and its particle size was 180—250 μm. PEG 6000 and the other powders were added to the fluidized-bed, and then the inlet temperature and the shaking/interval time were set at 85 °C and 2 s/15 s, respectively. The air flow rate was adjusted to 1 m/s. The powders were heated and held for 10 min when the powder bed temperature reached 65 °C, after which the powders were cooled to 40 °C.

Measurement of the Size Distribution and the Mean Diameter of Granules Prepared by FHMG Sieve analysis was carried out using a rotap shaker (Iida Seisakusyo Co. Ltd., Osaka, Japan). Granules were sieved with 150, 180, 250, 355, and 500 μm sieves. Then the size distribution and the mean diameter of the granules were calculated from the log-normal distribution equation.

Characterization of PEG 6000 The solidifying temperature of PEG 6000 was determined by using a differential scanning calorimeter (DSC-7, Perkin-Elmer Corp., CT, U.S.A.). The instrument was calibrated with an indium standard before measurement. Approximately 10 mg samples were weighed and sealed in aluminum pans. The samples were heated to 80 °C and cooled to −20 °C at a rate of 10 °C/min. Scanning was done under a nitrogen purge at a heating rate of 5 °C/min.

The viscosity of molten liquid PEG 6000 was measured at 98.89 °C (210 F) by using a Cannon–Fenske viscometer according to the JIS K-2283 method. PEG 400 was used as the outer medium.

The mean molecular weight of PEG 6000 was measured by the gel permeation chromatography (GPC) method (column: TSK gel G 6000 PW_{XL} + G 3000 PW_{XL}, 7.8 mm i.d.×60 cm, column temperature: 40 °C, mobile phase: 50 mmol/l NaCl, flow rate: 1.0 ml/min, injection volume: 200 μl).

PEG 6000 (5 g) was dissolved in 100 ml of purified water, and then the pH was determined with a pH meter.

Isothermal Crystallization of PEG 6000 DSC (DSC-7, Perkin-Elmer Corp., CT, U.S.A.) was used to investigate the isothermal crystallization behavior of molten PEG 6000. Approximately 10 mg samples were weighed and sealed in aluminum pans. In order to crystallize PEG 6000 at the target temperature under the supercooling state as correctly as possible, the samples were heated and held at 80 °C for 5 min, and then were flush cooled to 40, 43, and 45 °C at a cooling rate of −200 °C/min using liquid nitrogen. Isothermal crystallization was done each temperature and the process of crystallization was analyzed by the Hancock–Sharp method.[23] The most common and widely applicable kinetic equation for solid-state decomposition was described by Avrami–Erofeev[22] as follows:

$$\alpha = 1 - \exp(-Bt^m) \quad (1)$$

where α is the ratio of transition at time t, B is the constant, and m is the intrinsic value obtained from the theoretical equation for solid-state decomposition. α was determined by measuring the area under the crystallization peak of DSC profile at each temperature. Equation 1 can be written as

$$\ln[-\ln(1-\alpha)] = \ln B + m \cdot \ln t \quad (\alpha = 0.15 \sim 0.5) \quad (2)$$

When the slope m is calculated from the plot of $\ln[-\ln(1-\alpha)]$ *versus* $\ln t$, the mechanism of solid-state decomposition can be classified by referring to Table 2. The isothermal crystallization time (ICT) was defined as the time for complete solidification and was determined from the DSC profile.

Hot Stage Microscopy To observe its crystallization behavior, molten PEG 6000 was monitored and recorded using a hot stage microscopy system (FP84HT, Mettler Toledo, Switzerland) with a polarized filter. Molten PEG 6000 was cooled at a rate of −2 °C/min by controlling the temperature of the hot stage.

Powder X-Ray Diffraction (XRD) A powder X-ray diffractometer (MXP-3, MAC Science, Tokyo, Japan) was used to characterize the crystalline properties of PEG 6000. Samples were exposed to Cu-$K\alpha$ radiation under 35 kV and 20 mA over the 2θ range from 10° to 40° at increments of 2°/min.

Scanning Electron Microscopy (SEM) Granules were mounted on SEM sample-stubs using double-faced adhesive tape and were coated with gold–palladium. Observation was carried out at a voltage of 15 kV on an SEM instrument (JSM-5600LV, JEOL Ltd., Tokyo, Japan).

Table 1. Formulations Used for Fluidized Hot-Melt Granulation (FHMG)

Component	Composition (%)		Remarks
Cetraxate hydrochloride	60		Mean diameter: 20 μm
Lactose		60	DMV 450M
Polyethylene glycol 6000	25	25	PEG 6000, 180—250 μm fraction
Corn starch	13	13	
Talc	2	2	
Total	100	100	

Table 2. Kinetic Equations and Values of m[a)] for the Most Common Mechanisms of Solid-State Decomposition

Symbol	Equation	m	Mechanism
R_1	$\alpha = kt$	1.24	Zero-order mechanism (Polany–Winger equation)
R_2	$1-(1-\alpha)^{1/2} = kt$	1.11	Phase boundary reaction, cylindrical symmetry
R_3	$1-(1-\alpha)^{1/3} = kt$	1.07	Phase boundary reaction, spherical symmetry
F_1	$-\ln(1-\alpha) = kt$	1.00	Random nucleation, one nucleus on each particle
A_2	$[-\ln(1-\alpha)]^{1/2} = kt$	2.00	Random nucleation, two-dimensional growth of nuclei (Avrami–Erofeev equation)
A_3	$[-\ln(1-\alpha)]^{1/3} = kt$	3.00	Random nucleation, three-dimensional growth of nuclei (Avrami–Erofeev equation)
D_1	$\alpha^2 = kt$	0.62	One-dimensional diffusion
D_2	$(1-\alpha)\cdot\ln(1-\alpha)+\alpha = kt$	0.57	Two-dimensional diffusion
D_3	$[1-(1-\alpha)^{1/3}]^2 = kt$	0.54	Three-dimensional diffusion (Jander equation)
D_4	$(1-2\alpha/3)-(1-\alpha)^{2/3} = kt$	0.57	Three-dimensional diffusion (Ginstling–Brounshtein equation)

a) $\ln[-\ln(1-\alpha)] = \ln B + m \cdot \ln t$ ($\alpha = 0.15 \sim 0.50$).

Table 3. Characteristics of PEG 6000

Lot	Solidifying temperature (°C)	Mean diameter (μm)		OH-value	Mean molecular weight	Viscosity (mm^2/s)	pH
		D_{50}	σg				
A	58.1	200	1.1	12.6	8905	810.8	7.3
B	57.9	192	1.2	12.5	8976	802.1	7.2
C	58.6	197	1.2	12.4	9048	827.0	7.1
D	58.2	200	1.1	12.5	8976	826.4	7.2
E	58.1	191	1.1	12.5	8976	801.4	7.1
F	58.0	193	1.1	13.1	8565	793.6	7.2

Results and Discussion

FHMG FHMG is recognized as a novel and a simple method of making granules with a small size distribution. Haramiishi *et al.* investigated the formulation and mechanism of FHMG.[9] They reported that there was an optimum ratio between the powder and the melting material to obtain mononucleic particles by FHMG, which was related to the specific surface area and weight.[9] In this study, PEG 6000 was fixed at the optimum amount of 25 w/w % to obtain the highest yield of fine granules and the lowest amount of 150 μm pass (%). The other materials used, apart from PEG 6000, were all from the same lots to avoid inter-lot variations.

Various characteristics of the six lots of PEG 6000 used in this study are summarized in Table 3. No marked inter-lot differences of physical properties were observed. There were also no significant differences of the powder X-ray diffraction patterns of PEG 6000. After FHMG was done using CET as the active drug, however, a marked difference in the amount of 150 μm pass (%) was observed (Fig. 1). The content of CET under 150 μm was approximately 145% of the ideal amount, which means the labeled amount of CET/g. Lots A and B showed a smaller fine particle fraction compared with lots of C, D, E, and F. When lactose with the same mean diameter was used instead of CET, almost the same tendency of the amounts of particles under 150 μm (%) were obtained, as shown in Fig. 1. When the heating and cooling processes during granulation were observed in detail, it was found that fine powder was generated during the solidification process. Since no significant inter-lot differences of the physicochemical properties of PEG 6000 were observed, we focused on the solidification of PEG 6000. Using DSC, Larhrib and Wells demonstrated differences in the compression properties of PEG 10000 after thermal treatment.[24] Therefore, to clarify the influence of differences between lots of PEG 6000, the solidifying properties of each lot were evaluated by using DSC.

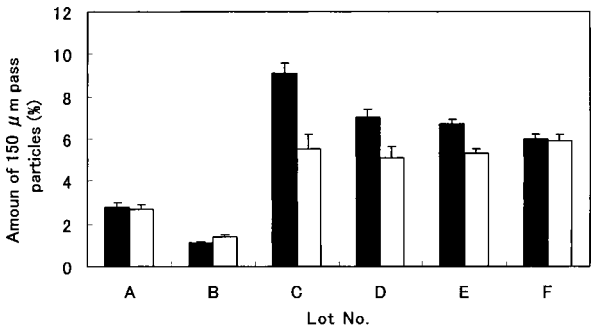

Fig. 1. Amount of 150 μm Pass Particles (%) in Granules Made with a Different Lots of PEG 6000 ($n=3$)

■: CET, □: lactose.

Characteristics of PEG 6000 Generally, it is known that a supercooling phenomenon will be observed during the solidification of polymers like PEG 6000 and this phenomenon was observed for molten PEG 6000. To clarify the solidification properties of PEG 6000, isothermal crystallization was investigated by DSC at a cooling rate of −200 °C/min. Figure 2 shows the isothermal crystallization profile of Lot B, which yielded the smallest amount of fine particles (150 μm pass). When the isothermal crystallization temperature was set at 40, 43 and 45 °C, the ICT was 0.7 min, 1.7 min, and 3.0 min, respectively. As the isothermal crystallization temperature became higher, the ICT tended to become longer. On the other hand, the isothermal crystallization profile of Lot C, which yielded the largest amount of fine particles (150 μm pass), is shown in Fig. 3. At every isothermal crystallization temperature, PEG 6000 was rapidly crystallized and the ICT was under 1 min. From these results, it was found that Lots C, D, E, and F of PEG 6000, which yielded relatively large amounts of 150 μm pass (%) after FHMG, had considerably shorter ICTs than Lots A and B during isothermal crystallization. Table 4 shows a comparison of the lots classified by slow or rapid crystallization. However, no marked differences of the physicochemical parameters were observed.

The heat of fusion (ΔH) during isothermal crystallization at 40, 43, and 45 °C was investigated for each lot of PEG 6000. Lots A and B were defined as showing slow crystallization, whereas Lots C, D, E, and F were defined as showing rapid crystallization. A summary of the ΔH values of PEG 6000 during isothermal crystallization is shown in Table 5. No significant difference of ΔH values was observed between PEG 6000 lots showing slow or rapid crystallization. These results were consistent with the X-ray diffraction patterns of the PEG 6000 lots before melting and after crystallization. It was concluded that the crystalline form of PEG 6000 was the same for slow and rapid crystallization.

The crystallization process of PEG 6000 under isothermal conditions were analyzed by the Hancock–Sharp method,[23] which can be applied to understand the transition of polymorphic forms[25] or crystallization.[26] With this method, the slope m estimated by plotting $\ln[-\ln(1-\alpha)]$ against $\ln t$ according to Eq. 2 is used in order to distinguish the reaction mechanism:

$$\ln[-\ln(1-\alpha)]=\ln B+m\cdot\ln t \quad (2)$$

where α is the fraction of transition and B is a constant. The

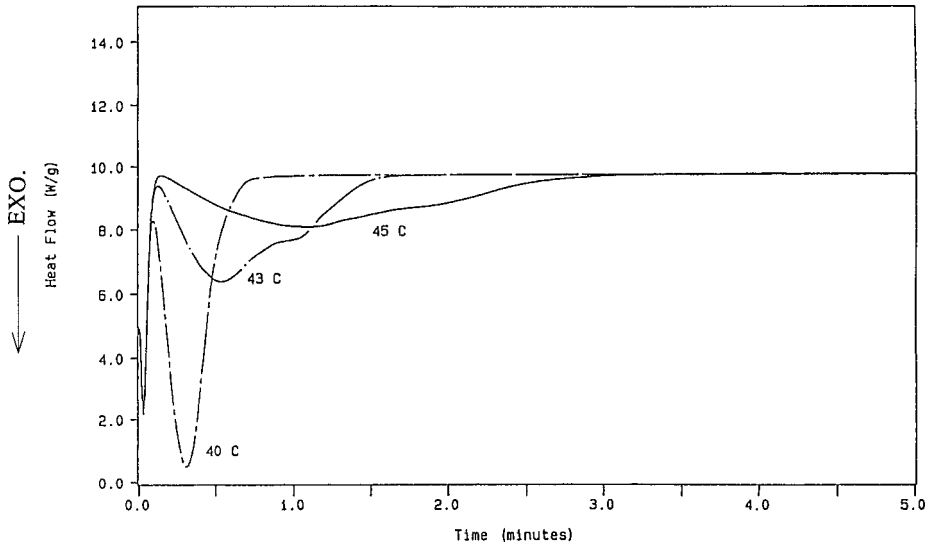

Fig. 2. Isothermal Crystallization Curves of PEG 6000 at 40, 43, and 45 °C
Lot: B, cooling rate: −200 °C/min.

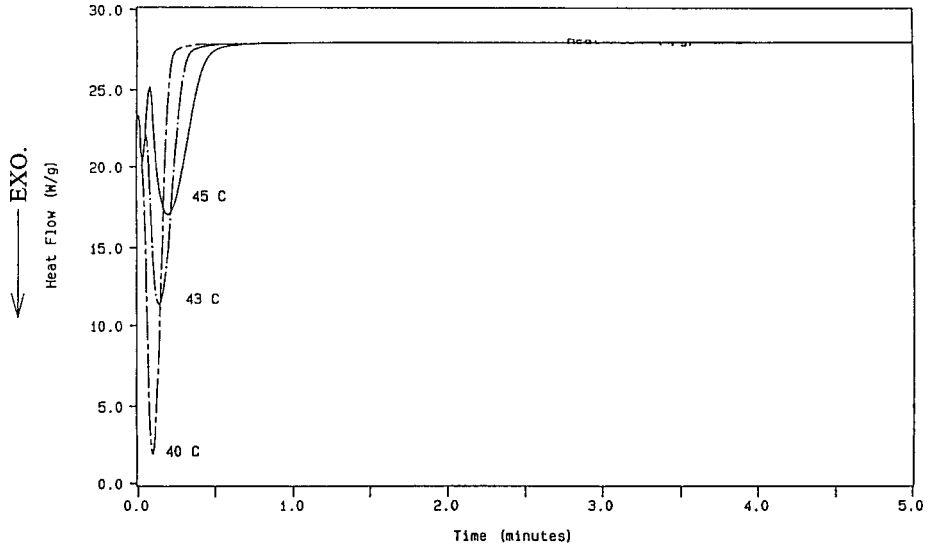

Fig. 3. Isothermal Crystallization Curves of PEG 6000 at 40, 43, and 45 °C
Lot: C, cooling rate: −200 °C/min.

Table 4. Characteristics of PEG 6000 Showing Slow or Rapid Crystallization

Classification	Lot	Solidifying temp. (°C)	Mean diameter (μm)		OH-value	Mean molecular weight	Viscosity (mm^2/s)	pH
			D_{50}	σg				
Slow	A, B	58.0±0.1	195.0±4.4	1.1±0.1	12.7±0.3	8815±220	802.2±8.6	7.2±0.1
Rapid	C—F	58.3±0.3	196.0±4.6	1.1±0.1	12.5±0.1	9000±42	818.3±14.6	7.1±0.1

value of *m* is an intrinsic value determined from various theoretical equations for solid-state decomposition. The results for Lot B (slow crystallization) and Lot C (rapid crystallization) are shown in Figs. 4 and 5, respectively. Every plot showed good linearity. The Hancock–Sharp constant (*m*) of PEG 6000 lots with slow and rapid ICT was calculated by the least-squares method. The results suggested that PEG 6000 showing slow crystallization had an *m* value of 2.9±0.4 and occurred by the mechanism of three-dimensional growth of nuclei (A_3). On the other hand, the *m* value of PEG 6000 showing rapid crystallization was 2.1±0.1, indicating that crystallization followed the mechanism of the two-dimensional growth of nuclei (A_2).

Morphological observation of PEG 6000 during crystallization was also done. To observe crystallization behavior, molten PEG 6000 was monitored and recorded by using a hot stage microscopy system with a polarized filter. Figure 6a shows the crystallization of Lot B from a temperature of 48.5

Table 5. Heat of Fusion (ΔH) of PEG 6000 Obtained from Isothermal Crystallization

Classification	Lot	ΔH (J/g) (Mean±S.D.)		
		40 °C	43 °C	45 °C
Slow	A, B	168±7	166±4	161±4
Rapid	C—F	172±8	168±7	167±4

to 42.9 °C. At 48.5 °C, only one crystal nucleus was seen in the field of view, and it was recognized that the nucleus grew slowly to form a large crystal. On the other hand, many nuclei were observed in the sample of Lot C at the same temperature at 48.5 °C, and many small crystals were seen in the field of view (Fig. 6b). At the end of the crystallization process at 42.9 °C, many cracks between crystals were observed due to the effect of crystal growth. It was thought that the amount of fine particles under 150 μm was determined at the time of solidification during FHMG because of the creation of cracks between PEG 6000 crystals.

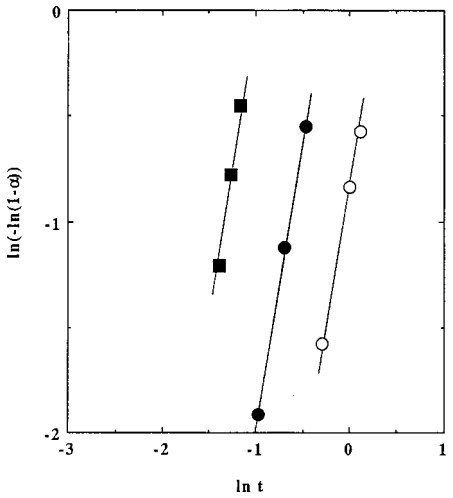

Fig. 4. Hancock–Sharp Plots for Isothermal Crystallization of PEG 6000 (α=0.15∼0.50)

Lot: B. ○: 45 °C (r=0.999), ●: 43 °C (r=0.999), ■: 40 °C (r=0.998).

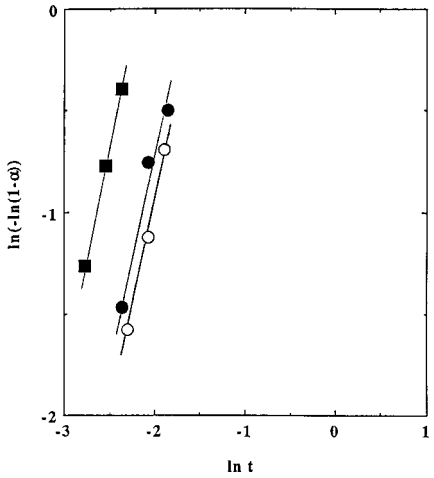

Fig. 5. Hancock–Sharp Plots for Isothermal Crystallization of PEG 6000 (α=0.15∼0.50)

Lot: C. ○: 45 °C (r=0.998), ●: 43 °C (r=0.966), ■: 40 °C (r=0.999).

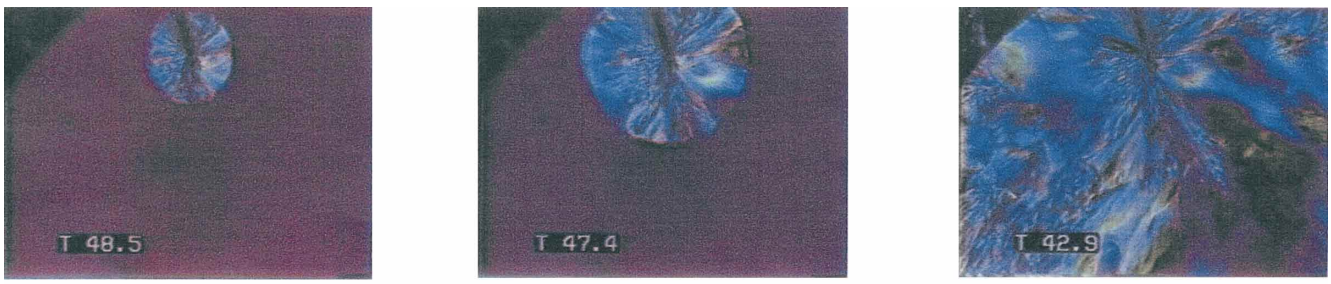

(a) Lot: B (×100)

(b) Lot: C (×100)

Fig. 6. Photo Micrographs of PEG 6000 during Crystallization (Magnification: ×100)

Each number in the photo shows the temperature at that time. (a) Lot: B, (b) Lot: C.

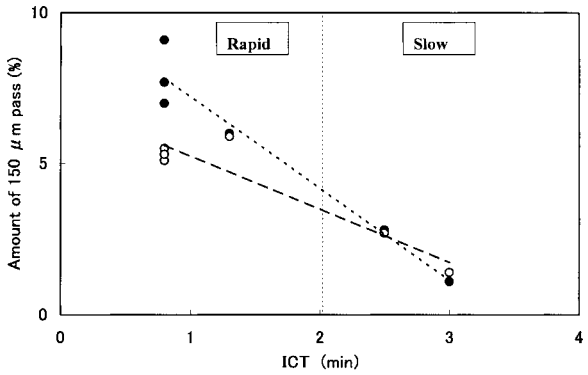

Fig. 7. Effect of the ICT of PEG 6000 at 45 °C on the Amount of 150 μm Pass Particles (%) after FHMG

●: CET, ○: lactose. Lots of PEG 6000 are the same as those in Table 3.

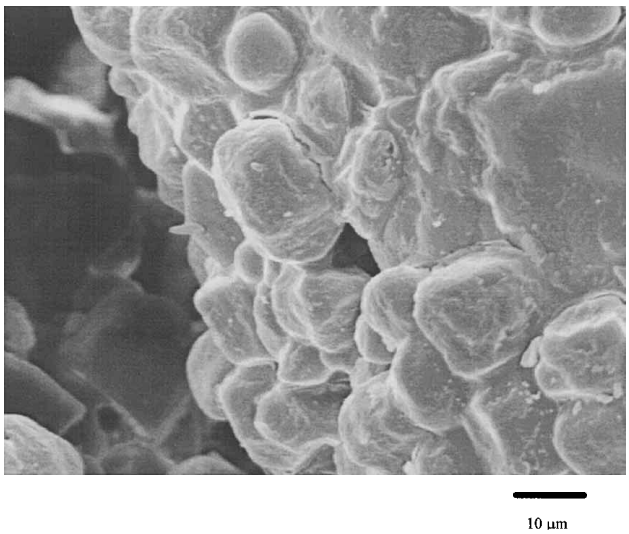

Fig. 8. SEM Photograph of Granules Having the Crack on the Surface Prepared by FHMG Containing PEG 6000 (Lot C, Magnification: ×1500)

Effect of Crystallization on the Properties of Granules

Based on the results obtained above, the relationship between the ICT and the amount of 150 μm pass (%) after FHMG using PEG 6000 is summarized in Fig. 7. It is obvious that the ICT of PEG 6000 affects the amount of fine particles after FHMG, since Lots A and B with a long ICT yielded fewer such particles compared with lots having a short ICT when using both CET and lactose as actives. When the amount of 150 μm pass (%) was plotted against the ICT of PEG 6000, a good correlation was observed using both CET and lactose (Fig. 7). Therefore, prediction of the amount of 150 μm pass (%) is possible by measuring the ICTs for CET and lactose. Moreover, PEG 6000 with an ICT of more than 2 min is preferable for FHMG. Generally, it is recognized that fewer fine particles is an advantage for taste masking coating or for packaging processes.

The morphological feature of granules obtained by FHMG were investigated using SEM. Figure 8 shows the surface of the granules containing Lot C. The crack on the surface of the granules is observed.

Thermodynamically, crystallization rate becomes larger when the difference of the free energy of PEG 6000 between the phases of the molten liquid and the crystalline caused by

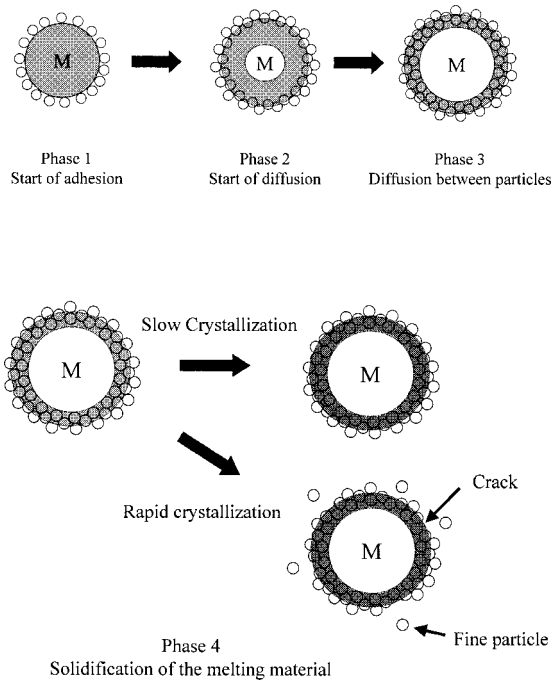

Fig. 9. Schematic Representation of the Mechanism of Fine Powder Generation from Mononucleic Granules during FHMG Method

M: Melting material.

the phase separation during the crystallization process increases. Therefore crystallization rate became larger when nuclei generated more, and ICT was considered to be shorter because of the two-dimensional growth of nuclei mechanism.

On the other hand, crystallization rate became smaller when nuclei generated fewer, and ICT was considered to be longer because of the three-dimensional growth of nuclei mechanism. After crystallization, cracks between the crystalline of PEG 6000 were generated more along with the discontinuous planes when crystallization rate was larger, since nuclei generated more.

From these results, the difference in the crystallization mechanism of PEG 6000 influenced the generation of the crack on the surface of the granules. Anti-adhesion of powder occurred at the point of crack during the crystallization of PEG 6000, and the amount of particle under 150 μm could be influenced.

A schematic representation of the mechanism of fine powder generation from mononucleic granules during FHMG is shown in Fig. 9. In phase 1, the meltable material (such as PEG 6000) begins to melt and an adhesion force acting on the particles is generated. In phase 2, the meltable material starts to diffuse between the powders adhering to its surface when the temperature exceeds its melting point. The molten material is diffused and spreads between the particles in phase 3. After heating, the granules are cooled below the solidifying temperature of the meltable material in phase 4. During solidification of the granules, the meltable material is crystallized. When the meltable material has a long ICT, powder adheres to the surface strongly during the crystallization process. However, if the meltable material has a short ICT, the powder does not adhere so well during cooling process of FHMG, since many cracks between PEG 6000 are generated on the surface of the granules after crystallization

due to the reduced sticking of particles on the surface of mononucleic granules.

Conclusions

The effect of the crystallization properties of PEG 6000 (used as a melting material) on mononucleic granules prepared by a novel FHMG method was investigated. It was found that PEG 6000 has two different crystallization mechanisms, one being two-dimensional growth of nuclei mechanism (A_2), the other being three-dimensional growth of nuclei mechanism (A_3). The amount of small particles (150 μm pass) in the granules showed a decrease with the increase of ICT. This indicates that a short ICT of PEG 6000 depending on its crystallization behavior may strongly affect on the particle size distribution and lead to decreased taste masking of granules. Therefore, the crystallization behavior of PEG 6000 for used in FHMG should be monitored. To reduce the amount of fine particle after FHMG, PEG 6000 having an ICT of more than 2 min at 45 °C should be used.

The results of this study also indicate that FHMG is a simple and a useful method of preparing granules without the need for solvents or water. However, the crystallization behavior of the melting material should be taken into account carefully.

Generally, it is well known that existence of a very small amount of impurities, or an addition of some ingredient, affects on the generation of crystal nuclei. However, it is still unclear what affects the crystallization behavior of PEG 6000. To identify the factors that modulate crystallization of PEG 6000, further studies are necessary.

Acknowledgements The authors would like to thank Dr. Takahiro Matsumoto of Daiichi Pharmaceutical Co., Ltd. for his helpful suggestions.

References

1) Bandelin F. J., "Pharmaceutical Dosage Forms: Tablets," Vol. 1, ed. by Lieberman H. A., Lachman L., Schwartz J. B., Marcel Dekker Inc., New York, 1989, pp. 131—194.
2) Matsunaga Y., Ohnishi Y., Bando N., Yuasa H., Kanaya Y., *Chem. Pharm. Bull.*, **45**, 1103—1107 (1997).
3) Ukita K., Murakami T., *Drug Dev. Ind. Pharm.*, **20**, 981—992 (1994).
4) Maejima T., Osawa T., Nakajima K., Kobayashi M., *Chem. Pharm. Bull.*, **45**, 518—524 (1997).
5) Maejima T., Osawa T., Nakajima K., Kobayashi M., *Chem. Pharm. Bull.*, **45**, 904—910 (1997).
6) Maejima T., Osawa T., Nakajima K., Kobayashi, M., *Chem. Pharm. Bull.*, **45**, 1332—1338 (1997).
7) Faham A., Prinderre P., Farah N., Eichler K. D., Kalantzis G., Joachim J., *Drug Dev. Ind. Pharm.*, **26**, 167—176 (2000).
8) Peck G. E., Anderson N. R., Banker G. S., "Pharmaceutical Dosage Forms: Tablets," Vol. 3, ed. by Lieberman H. A., Lachman L., Schwartz J. B., Marcel Dekker Inc., New York, 1990, pp. 1—76.
9) Haramiishi Y., Kitazawa Y., Sakai M., Kataoka K., *Yakugaku Zasshi*, **111**, 515—523 (1991).
10) Haramiishi Y., Kuroiwado M., Kitazawa Y., Proceed. of the 8th Symposium on Particulate Preparations and Designs, 1991, pp. 57—60.
11) Haramiishi Y., Funada A., Sasaki K., Shimizu T., Kitazawa Y., Suzuki T., Nakagami H., Proceed. of the 13th Symposium on Particulate Preparations and Designs, 1996, pp. 125—129.
12) Kitazawa Y., Nagao K., Mafune E., Hishida J., Kataoka K., Proceed. Intern. Symp. Control. Rel. Bioact. Mater., 1990, 17, S228.
13) Sunada H., Hasegawa M., Makino T., Sakamoto H., Fujita K., Tanino T., Kokubo H., Kawaguchi T., *Drug Dev. Ind. Pharm.*, **24**, 225—233 (1998).
14) Sunada H., Hasegawa M., Makino T., Fujita K., Sakamoto H., Tanino T., Kawaguchi T., *J. Soc. Powder Technol. Jpn.*, **33**, 481—486 (1996).
15) Kidokoro M., Haramiishi Y., Sagasaki S., Shimizu T., Yamamoto Y., *Drug Dev. Ind. Pharm.*, **28**, 67—76 (2002).
16) Schæfer T., Holm P., Kristensen H. G., *Acta Pharm. Nord.*, **4**, 133—140 (1992).
17) Schæfer T., Taagegaard B., Thomsen L. J., Kristensen H. G., *Eur. J. Pharm. Sci.*, **1**, 125—131 (1993).
18) Schæfer T., Holm P., Kristensen H. G., *Acta Pharm. Nord.*, **4**, 245—252 (1992).
19) Schæfer T., Mathiesen C., *Int. J. Pharmaceut.*, **139**, 125—138 (1996).
20) Schæfer T., Mathiesen C., *Int. J. Pharmaceut.*, **139**, 139—148 (1996).
21) Voinovich D., Moneghini M., Perissutti B., Franceschinis E., *Eur. J. Pharm. Biopharm.*, **52**, 305—313 (2001).
22) Avrami M., *J. Chem. Phys.*, **7**, 1103—1112 (1939).
23) Hancock D. J., Sharp J. H., *J. Am. Ceram. Soc.*, **55**, 74—77 (1972).
24) Larhrib H., Wells J. I., *Int. J. Pharmaceut.*, **153**, 51—58 (1997).
25) Umeda T., Ohnishi N., Yokoyama T., Kuroda T., Kita Y., Kuroda K., Tatsumi E., Matsuda Y., *Chem. Pharm. Bull.*, **33**, 2073—2078 (1985).
26) Otsuka M., Kaneniwa N., *Chem. Pharm. Bull.*, **36**, 4026—4032 (1988).